USGS Award No.: 99HQGR0049

HAYWARD FAULT SUBSURFACE SLIP FROM JOINT ANALYSIS OF MICROEARTHQUAKE RECURRENCE AND SPACE GEODESY

Thomas V. McEvilly and Roland Burgmann (University of California at Berkeley)

Author and affiliation:
Robert M. Nadeau
Berkeley Seismological Laboratory
University of California, Berkeley
215 McCone Hall, MC: 4760,
Berkeley, CA 94720−4760
Tel: (510) 643−3980
Fax: (510) 643−5811
e−mail: nadeau@seismo.berkeley.edu

Non−Technical Project Summary

This project addresses the seismic potential and natural hazard presented by the Hayward, Calaveras and Mission faults to the San Francisco Bay area through the use of fault creep, space−based technology (i.e. GPS and InSAR) and high−resolution observations of characteristic microearthquake activity. It provides detailed information on the magnitude of subsurface aseismic fault slip and it's variation in space and time. Results directly contribute to reducing losses from earthquakes in the San Francisco Bay area by contributing reliable estimates of earthquake potential (size and slip−deficit accumulation rates of locked fault segments) along three major fault segments in the region.

FINAL TECHNICAL REPORT
USGS Award No.: 99HQGR0049

HAYWARD FAULT SUBSURFACE SLIP FROM JOINT ANALYSIS OF MICROEARTHQUAKE RECURRENCE AND SPACE GEODESY

Program Elements: **I**

Principal Investigator:
Thomas V. McEvilly (deceased) and
Roland Burgmann
Berkeley Seismological Laboratory
University of California, Berkeley
215 McCone Hall, MC: 4760,
Berkeley, CA 94720−4760
Tel: (510) 643−9545
Fax: (510) 643−5811
e−mail: burgmann@seismo.berkeley.edu

Recipient:
University of California − Berkeley

Research supported by the U.S. Geological Survey (USGS), Department of the Interior, under USGS award number 01HQGR0066. The views and conclusions contained in this document are those of the authors and should not be interpreted as necessarily representing the official policies, either expressed or implied, of the U.S. Government.

USGS Award No.: 99HQGR0049

HAYWARD FAULT SUBSURFACE SLIP FROM JOINT ANALYSIS OF MICROEARTHQUAKE RECURRENCE AND SPACE GEODESY

Thomas V. McEvilly and Roland Burgmann (University of California at Berkeley)

Author and affiliation:
Robert M. Nadeau
Berkeley Seismological Laboratory
University of California, Berkeley
215 McCone Hall, MC: 4760,
Berkeley, CA 94720−4760
Tel: (510) 643−3980
Fax: (510) 643−5811
e−mail: nadeau@seismo.berkeley.edu

ABSTRACT

This project addresses the seismic potential and natural hazard presented by the Hayward, Calaveras and Mission faults (HF, CF and MF, respectively) to the San Francisco Bay area through the use of fault creep and space−based technology (i.e. GPS and differential radar interferometry (InSAR)) combined with high−resolution observations of characteristic microearthquake activity on the faults. This research provides detailed information on the magnitude of subsurface aseismic fault slip and it's variation in space and time. Results directly contribute to reducing losses from earthquakes in the San Francisco Bay area by contributing reliable estimates of earthquake potential (size and slip−deficit accumulation rates of locked fault segments) along three major fault segments in the region.

Imaging distributed slip on subsurface faults from surface displacements is a difficult task, plagued by limits in the spatial resolution of the surface displacements and ambiguities in the depth resolution of slip variations. The ability to derive even just a few point measurements of fault slip at depth adds invaluable constraints on the spatial distribution and magnitude of aseismic slip along fault surfaces. Therefore, inversions aided by such deep constraints can significantly sharpen the resolution of locked patches along the Hayward (HF), Calaveras (CF) and Mission (MF) faults. Subsurface slip−rate estimates from sequences of characteristically repeating microearthquakes (CS) can be integrated with surface and space based geodetic measurements in inversions in a straightforward manner. We have successfully applied joint geodetic and repeating earthquake techniques to the northern HF using INSAR, GPS, creep and NCSN archival data (*Bürgmann et al.,* 2000). And we are expanding our analysis to image the deep slip behavior of the HF, MF and CF system. Using the newly released double−difference earthquake relocation code hypoDD, we are also resolving the relative seismic structure of these East−Bay faults in much greater detail, which provides important information about the sub−

surface fault geometry, especially in the Mission stepover region linking the HF and CFs. We now have preliminary CS slip rate estimates for a sparse distribution of CS along an 100 km extent of the HF−MF−CF system. The preliminary slip rate estimates appear consistent with independent deformation measurements and appear to resolve accelerated slip transients, such as those following the 1984 Morgan Hill earthquake along the CF. No CS events are found in the bifurcation region of the MF and northern CF nor at depths > 6 km along the southern HF. Densification of the CS catalog is currently underway and a mapping of aseismic fault slip at depth and through time is being compiled based on the joint inversion of all available data.

USGS Award No.: 99HQGR0049

HAYWARD FAULT SUBSURFACE SLIP FROM JOINT ANALYSIS OF MICROEARTHQUAKE RECURRENCE AND SPACE GEODESY

Thomas V. McEvilly and Roland Burgmann (University of California at Berkeley)

Author and affiliation:
Robert M. Nadeau
Berkeley Seismological Laboratory
University of California, Berkeley
215 McCone Hall, MC: 4760,
Berkeley, CA 94720−4760
Tel: (510) 643−3980
Fax: (510) 643−5811
e−mail: nadeau@seismo.berkeley.edu

NON−TECHNICAL ABSTRACT

This project addresses the seismic potential and natural hazard presented by the Hayward, Calaveras and Mission faults (HF, CF and MF, respectively) to the San Francisco Bay area through the use of fault creep and space−based technology (i.e. GPS and differential radar interferometry (InSAR)) combined with high−resolution observations of characteristic microearthquake activity on the faults. This research provides detailed information on the magnitude of subsurface aseismic fault slip and it's variation in space and time. Results directly contribute to reducing losses from earthquakes in the San Francisco Bay area by contributing reliable estimates of earthquake potential (size and slip−deficit accumulation rates of locked fault segments) along three major fault segments in the region.

Imaging distributed slip on subsurface faults from surface displacements is a difficult task, plagued by limits in the spatial resolution of the surface displacements and ambiguities in the depth resolution of slip variations. The ability to derive even just a few point measurements of fault slip at depth adds invaluable constraints on the spatial distribution and magnitude of aseismic slip along fault surfaces. Therefore, inversions aided by such deep constraints can significantly sharpen the resolution of locked patches along the Hayward (HF), Calaveras (CF) and Mission (MF) faults. Subsurface slip−rate estimates from sequences of characteristically repeating microearthquakes (CS) can be integrated with surface and space based geodetic measurements in inversions in a straightforward manner. We have successfully applied joint geodetic and repeating earthquake techniques to the northern HF using INSAR, GPS, creep and NCSN archival data (*Bürgmann et al.*, 2000). And we are expanding our analysis to image the deep slip behavior of the HF, MF and CF system. Using the newly developed earthquake relocation techniques, we are also resolving the relative seismic structure of these East−Bay faults in much greater detail, which provides important information about the sub−surface fault

geometry, especially in the Mission stepover region linking the HF and CFs. We now have preliminary CS slip rate estimates for a sparse distribution of CS along an 100 km extent of the HF−MF−CF system. The preliminary slip rate estimates appear consistent with independent deformation measurements and appear to resolve accelerated slip transients, such as those following the 1984 Morgan Hill earthquake along the CF. No CS events are found in the bifurcation region of the MF and northern CF nor at depths > 6 km along the southern HF. Densification of the CS catalog is currently underway and a mapping of aseismic fault slip at depth and through time is being compiled based on the joint inversion of all available data.

FINAL TECHNICAL REPORT: HAYWARD FAULT SUBSURFACE SLIP FROM JOINT ANALYSIS OF MICROEARTHQUAKE RECURRENCE AND SPACE GEODESY

Table of Contents:

FINAL TECHNICAL REPORT: HAYWARD FAULT SUBSURFACE SLIP FROM JOINT ANALYSIUS OF MICROEARTHQUAKE RECURRENCE AND SPACE GEODESY

Robert M. Nadeau (University of California at Berkeley)

Introduction

The faults along the eastern side of San Francisco Bay are arguably some of the most hazardous faults in the world when one considers the probability of an earthquake together with the density and nature of development along them. The M~7 October 21, 1868 Hayward Fault (HF) earthquake produced a 30−to−40−km−long surface rupture, and slip of up to 2 m may have extended at depth from Warm Springs to near Berkeley (Yu and Segall, 1996). No other large historic earthquake has been unequivocally assigned to the HF. An 1836 earthquake, long assumed to have ruptured the northern HF, may actually have occurred on the San Andreas fault to the south, implying that the northernmost HF has not ruptured for at least 220 years (Toppozada and Borchardt, 1998). Williams (1992) documents at least six HF ruptures during the past 2100 years in a trenching study on the southern HF. Some additional paleoseismic constraints exist for the Calaveras fault (CF) (e.g., Kelson et al., 1996). however, earthquake hazard estimates on the East Bay faults are complicated by the observation of aseismic slip along their length, which directly affects earthquake potential estimates and makes paleoseismic excavations more difficult to interpret.

Long−term HF slip rate estimates of ~10 mm/yr. Suggest that more than a meter (>2 m on northern HF) of slip potential has accumulated since the most recent events, making the HF potentially capable of M?6.5 events in the near future (Lienkaemper et al., 1991; Savage and Lisowski, 1992; Simpson et al., 2001). Accordingly, the HF has been assigned the highest probability for a destructive earthquake in the Bay area in the next 30 years with an estimated recurrence interval of 167 +/− 67 years (WGCEP, 1999). Estimated cost and loss of life from such an event approaches 10s of billions of dollars and several thousand deaths, respectively. At present the seismologic community knows very little about the segmentation of East−Bay faults, the distribution of locked and creeping segments in the subsurface, and the role of the Mission fault (MF) step−over in transferring fault loading between the CF and HF.

This project addresses the seismic potential and natural hazard presented by the HF, CF and MF to the San Francisco Bay area through the use of space−based technology, namely GPS and differential radar interferometry (InSAR), combined with high−resolution observations of characteristic microearthquake activity and creep on the faults. Our results can be applied directly to the development of much improved earthquake forecast and hazard models and to strong ground motion source models since they provide more precise information on the size, segmentation, and loading rate histories on the expected segments of rupture along the HF, CF and MF. Since these faults exist in heavily populated regions of the Bay Area, such information will be invaluable in the planning and building of structures resistant to damage resulting from earthquakes. Results provide detailed information on the magnitude of subsurface aseismic fault slip and it’s variation in space and time. This project directly contributes to reducing losses from earthquakes in the San Francisco Bay area by contributing reliable estimates of earthquake potential (size and slip−deficit accumulation rates of locked fault segments) along the three major fault segments.

Imaging distributed slip on subsurface faults from surface displacements is a difficult task, plagued by limits in the spatial resolution of the surface displacements and ambiguities in the depth resolution of slip variations. The ability to derive even just a few point measurements of fault slip at depth adds invaluable constraints on the spatial distribution and magnitude of aseismic slip along fault surfaces. Therefore, inversions aided by such deep constraints can significantly sharpen the resolution of locked patches along the HF, CF and MF. Previously we successfully applied joint geodetic and repeating earthquake techniques to the northern HF using INSAR, GPS, creep and NCSN archival data (*Bürgmann et al.*, 2000). And we have begun to expand our analysis to image the deep slip behavior of the HF, MF, and CF system. Using the newly released double−difference earthquake relocation code hypoDD, we are also resolving the seismic structure of these East−Bay faults in much greater detail, which provides important information about the sub−surface fault geometry, especially in the Mission stepover region linking the HF and CF. We now have preliminary repeating−event slip rate estimates for the the HF−MF−CF system in the East−Bay. The preliminary slip rate estimates appear consistent with independent deformation measurements and appear to resolve accelerated slip transients, such as following the 1984 Morgan Hill earthquake along the CF. No repeating events are found at the bifurcation of the MF and northern CF nor at depths > ~6 km along the southern HF.

Scientific Significance. Achieving greater understanding of the HF, CF and MF systems is a scientific challenge, requiring the integration of a wide range of observations and scientific methods. The HF is creeping yet presumably accumulating strain for M6.5+ earthquakes at recurrence rates possibly less than 200 yrs. Recurrence interval estimates and potential magnitudes of earthquakes along the CF and MF are highly variable and little is known about the geometry, seismogenic character and earthquake scenarios for the Mission Hills area. Patterns of hypocenters along these faults exhibit clustering into pockets and lineations of activity both separated by gaps. The base of seismicity at 10−13 km, is more shallow along the HF than to the east or west. There are similar ’multiplet’ events within the seismicity on all three faults, which allow for the application of our technique for estimating slip rates at depth using existing waveform data. (*Nadeau*, 1995; *Nadeau and Johnson*, 1998; *Nadeau and McEvilly*, 1999 and 2000). InSAR is considered the most significant observational advance in crustal deformation research since the development of GPS and the integrated use of both techniques with available creep information promises to revolutionize our ability to examine fault zone processes along these faults at depth and in greater detail.

This study applies new methods for formally combining geodetic and seismological observations on the HF, CF, and MF zones to determine the distribution of slip on the fault throughout the subsurface. The research has resulted in the determination of fault kinematic parameters that are crucial for earthquake hazard assessment, and contributes to improved understanding of the mechanics of aseismic and seismic slip along strike−slip faults in the Bay Area. Geodetic and seismic data suggest that partially creeping faults behave in a strongly time−dependent fashion including the occurrence of slow earthquakes (*Linde et al.*, 1996), a ’pulsing’ of slip rates over several years (*Nadeau and McEvilly*, 2000), and a complex response of creeping faults to regional stress changes (*Lienkaemper et al.*, 1997, *Bürgmann et al.*, 1997, 1998; *Schmidt* *and Bürgmann*, 1998 and manuscript in preparation, *Wilber and Bürgmann*, 1999). Our ability to constrain the development of subsurface aseismic fault slip over several years at heretofore unrivaled resolution is providing a rich database that will allow for new advances in the theoretical understanding of fault mechanics.

Technological Significance. This research is providing technical advances in GPS deformation monitoring, InSAR and earthquake data analysis directed toward determination of the distribution of slip on seismogenic faults in space and time, incorporating a new class of earthquake data. New and evolving techniques in InSAR analysis (e.g., time series integration, permanent scatterer analysis, and pixel resampling strategies), double−difference earthquake relocations (*Waldhauser et al.*, 1999), the analysis of characteristically repeating microearthquakes (e.g., detection automation, integration of local borehole networks, and rate calibration) and inverse modeling (e.g., InSAR covariance structure, data type integration, variable smoothing constraints, and resolution analysis) are being developed and incorporated into our analysis to provide heretofore unequaled resolution of the geometry and spatial distribution of aseismic slip on the East Bay faults. This project is using these new methods and the accumulating data in new ways to better define the deformation on and interaction between these faults through space and time. The integration of all available INSAR data (>150 interferograms), the reduction of GPS velocity uncertainties using observation periods equal to or larger than 3 years, and the addition of dozens of multiply repeating characteristic miroearthquake sequences is providing an unequaled picture of the distribution and changes of aseismic slip along the East−Bay faults.

Data, Inversion and Results

We have developed the appropriate tools to jointly invert four types of measurements (GPS, InSAR, surface creep, and characteristic microearthquake recurrence rates) to determine the distribution of aseismic creep and locked segments along faults, at the surface and at depth. This project has focused on (1) inclusion of all available data, (2) complete coverage of the HF−MF−CF system in the East−Bay, and (3) careful analysis of data uncertainties and noise sources required for a successful model analysis. In addition to the deformation measurements, it is crucial to have an accurate representation of the 3D geometry of the slipping faults. Analysis of relocated micro−earthquakes (using the USGS HypoDD code) are showing significant off−vertical dips, especially along the MF stepover region, and short lived transients of seismicity on short fault segments splaying off of the CF following the 1984 Morgan Hill event.

Surface creep measurements. Until recently, surface creep measurements have provided the primary constraint on model evaluations of the seismic potential along the Hayward fault (e.g., *Savage and Lisowski*, 1993). Existing creepmeters along the Hayward fault and Calaveras fault (*Langbein*, pers. comm.) and alignment array surveys (e.g., *Lienkaemper et al.*, 1997) provide important constraints on surface creep rates especially along the Hayward fault (*Lienkaemper et al.*, 2001). In addition to providing precise surface slip constraints for the model inversions, the horizontal creep measurements can be integrated with the InSAR range−change data to resolve vertical slip components in response to subsurface fault geometry and loading parameters and possible hydrological effects.

GPS Measurements. GPS data used in this study come from USGS, Stanford University, UC

Davis and UC Berkeley campaign measurements throughout the Bay area. *Manaker et al*. (manuscript submitted to *J. Geophys. Res.*) integrated GPS and EDM data to constrain distributed aseismic−slip models, and estimate the seismic potential along the Calaveras fault. The initial distribution of existing GPS sites near the HF and MF was too widely spaced to aid much in determining the depth of the creeping portion of the faults (*Bürgmann et al.*, 2000). Since 1999 we have added about 25 additional sites to our GPS network, primarily along the HF. We primarily relied on existing benchmarks from the NGS database of survey monuments as well as on sites established for alignment array creep measurements by J. Lienkaemper and J. Galehouse. We also integrate results from a 2−color EDM network occupied by John Langbein in the 1990s near the Mission fault with our GPS results. We have also added a few more continuously operating sites to the BARD monitoring network in the East Bay that will support our efforts. **Figure 1** shows the currently available horizontal station velocities along the East Bay faults. Based on current measurement precision we can project that with measurements through 2003, we will achieve near mm/yr velocity precisions at most of our sites, which are required for the objectives in this project. We are currently acquiring 7 new Trimble 5700 GPS receivers from UC Berkeley startup, which will be used for this project, complemented by receiver loans from UC Davis and Stanford University as needed.

<u>*InSAR Measurements.*</u> *Bürgmann et al.* (1998) demonstrated the feasibility of using InSAR to monitor shallow slip along the HF with data collected by the European Space Agency (ESA) ERS−1&2 spacecraft in 1992 and 1995. Next, we completed analysis of two 1992−1997 interferograms spanning the northern HF and performed a prototype inversion and joint analysis of InSAR,R creep, GPS, and repeating microearthquake data (*Bürgmann et al.*, 2000). The analysis revealed a potentially unlocked northern HF segment whose surface creep rate is reduced primarily by the pinning effects of the locked 1868 earthquake source region to the south (below ~ 5 km) and the tip of the creeping Hayward fault just offshore Point Pinole. **Figure 2** shows a 1992−2000 interferogram, with gray shaded zones indicating incoherent regions, where vegetation or erosion doesn't allow for interferometry. The Hayward fault is clearly visible as a step in the otherwise smoothly varying range change field.

We have recently begun the formal integration of now 171 interferograms covering the HF (*Schmidt et al.*, 2000; **Figure 3A**). In this approach, data from all the interferograms are formally combined in a least−squares inversion to determine a time series of range change at each image element (**Figure 3B**). This analysis can resolve transient deformation episodes (such as a large creep event on the southern Hayward fault, *Schmidt et al.*, 2000). This constitutes the most comprehensive and complete analysis of all available InSAR data yet.

As mentioned above, InSAR images of the Bay area are primarily coherent over urban developed regions, whereas undeveloped regions that are vegetated and have steep topography are not suitable for interferometry spanning time intervals of greater than about 1 year. This includes much of the East Bay Hills to the east of the HF, as well as much of the terrain along the Mission and Calaveras faults. We are currently evaluating the utility of the so−called permanent scatterer technique to allow for the inclusion of data in these regions (*Johanson and Burgmann,* 2001). This approach relies on methods to identify individual coherent pixels (such as buildings or outcrops) in an otherwise incoherent region. These permanent scatterers can then provide point measurements of range change throughout the area.

<u>*Slip Rate Measurements from Earthquake Recurrence.*</u> This method has been developed in our research program using data from another borehole network along an active fault zone.

Studies at very high resolution of microearthquakes at Parkfield, CA since 1987 revealed a systematic organization in space and time, dominated by spatial clustering of nearly identical, regularly recurring microearthquakes ('characteristic events') on small (meters to 10s of meters) wide patches within the fault zone (Nadeau et al., 1994, 1995; Nadeau and McEvilly, 1997). At Parkfield, nearly half of the 5000+ events in the 1987−1998 catalog exhibit this trait. In general, recurrence intervals (0.5 to 3 yr.) scale with the magnitude of the repeating events for the magnitude range available (Mw −0.7 to 3). Clusters of these characteristic events occur throughout the slipping fault surface. Scalar seismic moments were estimated for 268 microquakes contained in 53 repeating sequences and combined with equivalent estimates from 8 similar but larger event sequences from the Stone Canyon section of the fault and the main Parkfield M6 sequence. These estimates show that seismic moment is being released as a function of time in a very regular manner where repeating earthquakes occur and for a wide range of earthquake magnitude. Measurements of the moment release rate, combined with an assumed tectonic loading rate, lead to estimates of the seismic parameters source area, slip, and recurrence interval. Such parameters exhibit a systematic dependence upon source size over a range of 10^{10} in seismic moment, which can be described by simple scaling relationships (*Nadeau and Johnson*, 1998). What emerges from this analysis of moment release rates is a quantitative description of an earthquake process that is controlled by small strong asperities that occupy less than 1% of the fault area. A 26−months period of greatly increased activity during the study interval (M4.2, 4.6, 4.7 and 5.0 events and their aftershocks) accompanied changes exceeding 50% in previously stable recurrence intervals. *Langbein et al.* (1998) report on evidence in deformation measurements for a slip rate increase in 1993 at Parkfield. *Nadeau and McEvilly* (1999) show that it is possible under reasonable assumptions to infer the spatial distribution of variations in slip−rate on the fault surface from the changes in recurrence intervals for the characteristic event sequences. The analysis requires an assumption of constant area for the characteristic repeating sources − one easily supported by the lack of any appreciable change in the seismic moments and waveforms (over the 100 Hz bandwidth) associated with the change in recurrence interval. Results of our prototype study on the northern segment of the HF were encouraging and have been published in *Science* (*Bürgmann et al.*, 2000). We have subsequently found sufficient repeating earthquake activity along the HF and CF and MF to accomplish the proposed goals (**Figures** 4 **and 5**).

We have completed our initial and computationally intensive search for characteristic sequences on the southern HF, CF and MF, where seismicity resembles the Parkfield clustering, but at a lower rate. Our search for repeaters along the HF, MF and CF, despite reduced detection completeness (M~1.3) of NCSN, reveals large numbers of highly similar and repeating events (coherency > 0.95) in the NCSN catalog distributed widely on all three faults, indicating the presence of substantial repeating earthquake activity (**Figure 5**). Using NCSN surface data the fractions of identifiable repeaters to be about 10% 15% and 25%, for the northern HF, southern HF/MF and CF segments respectively. The lowest fractions are explainable in part by lower slip rates and higher magnitude thresholds, since under these conditions recurrence intervals may be longer than observation times. At Parkfield, where the slip rate is much higher and using NCSN data, the fraction of repeaters is about 48%. In our prototype analysis on the northern HF, we showed that sufficient information was available to resolve spatially varying features of slip using surface NCSN data but that monitoring of short−term temporal variations was not practical with the limited resolution of the surface data on such a slowly moving fault. To the southeast, on the faster moving MF and CF, we have found sufficient rates of quake repetition to allow us to use NCSN data for monitoring transients (**Figure 5**) as is currently being achieved on the faster slipping SAF to the West (Nadeau and McEvilly, 2000).

Fault Geometry and Deep Slip from Hayward, Calaveras, Mission and Quien Sabe Fault Seismicity. Using NCSN arrival times, we have relocated the seismicity along the HF−MF−CF system using the USGS relocation code HypoDD (**Figures 1 and 5)** and are evaluating the more highly resolved spatial and temporal seismicity patterns in relation to surface and spaced based deformation estimates, to the spatial and temporal distribution of repeating earthquake sequences and to the post−seismic period following the 1984 Morgan Hill earthquake. Our preliminary findings indicate that, as at Parkfield and on the creeping section of the SAF, the locations of repeating earthquake sequences are confined to the central portion of seismicity on large faults. However, repeating quakes are not ubiquitous on all faults. For example our search for characteristic quakes in our study region failed to identify any repeating sequences on the CF fault north of its juncture with the MF trend between Fremont and San Jose (**Figure 5)**. Furthermore, along the MF and southern HF, repeating sequences only appear in the shallow portion of the seismogenic zone (**Figure 5**, depth section) and their rate of repetition (indicated by their low, blue, slip rates) are low relative to the slip rates on the northern HF and CF segments. Since repeating earthquake activity requires repeated loading from the adjacent slipping fault, we interpret the regions of seismically active but non−repeating seismicity to be non−creeping and possibly locked and the low repeat rates of the shallow repeating sequences to be in response to the shielding effect of the deeper locked section of the southern HF and MF. If this is the case, high resolution relocations of repeating earthquake activity may prove a valuable tool for delineating locked fault segment boundaries in more detail at depth. Also of note in this regard is the lack of repeating earthquake activity on two splays of transient earthquake activity emanating from the CF south of San Jose. High precision relocations show that these splays were active during the post−seismic period following the Morgan Hill (MH) earthquake of 1984, but in subsequent years these splays have become aseismic (**Figure 5**, map view, 84−92.5 and 92.5 to 02). It is not yet clear if the lack of repeating sequences on these splays is due to a relatively minor amount of slip release on the faults after MH or to a fundamental instability in the strength properties of earthquake patches on these subsidiary faults.

In addition to the structural features manifest by the relocations and repeating earthquake analyses, temporal variations are also clearly evident. Shown in the right most panels of **Figure 5** are map views of the repeating sequences, color coded to their slip rate estimates. On the CF during the period 1984−1992.5 repeat rates (and inferred slip rates at depth) are very high in comparison to repeat rates for sequences from 1992.5 to 02. In addition, repeating events on the southern HF during the 6 years following the Loma Prieta earthquake nearly ceased, which agrees well with diminished surface deformation rates observed on this fault segment (*Lienkaemper et al.*, 1997; *Bürgmann et al.*, 1998).

We have also applied similar relocation and repeating earthquake techniques further south on the CF and Quien Sabe fault near the bifurcation of the SAF where little surface or space based deformation data is available. In this region, the seismic structure and repeat rates of the characteristic sequences indicates a very complicated and heterogeneous slip regime apparently due to complex fault geometry at depth, rapid slip transients initiated by moderate earthquakes, and the presence of a significantly greater fraction of locked (i.e. non−creeping) fault behavior (*Templeton et al.*, 2001) (**Figures 6 and 7**).

Inversion for Distributed Fault Slip. The increasingly densified and precise GPS and InSAR measurements along the HF, CF, and MF, together with surface and sub−surface creep measurements will yield greater detail on the distribution of creeping and locked segments of these faults. Precise mapping of the slip distribution along the faults will provide much improved and quantifiable constraints on their seismic potential. Surface deformation can be directly related to subsurface fault slip or other source mechanisms (e.g., *Harris and Segall*, 1987). We model the measured displacement field with rectangular displacement discontinuities (dislocations) in an isotropic, homogeneous and elastic half−space (*Okada*, 1985). A number of modeling and inversion tools have been developed that enhance our ability to model the various data types in a self−consistent and rigorous manner (e.g., *Bürgmann et al.*, 1997, 2000). Our inversions attempt to minimize the weighted residual sum of squares $WRSS = (d_{obs} - d_{mod})^T \times cov^{-1} \times (d_{obs} - d_{mod})$, where d_{obs} and d_{mod} are the observed and modeled motions and *cov* is the data covariance matrix. The GPS errors of the horizontal and vertical displacements are derived from the formal GPS−analysis uncertainties. The sub−sampled InSAR data were previously modeled as uncorrelated. With the additional InSAR data, it is now possible to stack interferograms in regions where the deformation rates appear linear. This procedure provides statistical information about the error structure in the InSAR data set and will allow us to properly weight both the InSAR and GPS data in the inversions. In addition to solving for the model fault parameters we also estimate a constant offset and two orbital tilt parameters (a linear slope across the interferogram) when including InSAR data. Surface, and sub−surface (repeater) creep estimates are included as additional slip constraints on adjoining slip patches, weighted depending on their variance estimates. The faults are subdivided into a grid of smaller fault elements and we determine the optimal slip vector on each patch. We commonly apply additional constraints to the inversions, such as applying smoothing and non−negativity (right−lateral only) constraints to the slip−distributed models. A finite difference approximation of the Laplacian imposes smoothness constraints on the slip distribution (*Harris & Segall*, 1987). We can apply additional edge constraints; for example slip at the NW end of the HF in the model in **Figure 9** is minimized.

Using surface deformation data collected in the San Francisco Bay area, we have applied this approach to develop models of deep slip rates on the whole SAF system (*Bürgmann et al.*, 1994), to model time−dependent and spatially variable slip following the Loma Prieta earthquake (*Bürgmann et al., 1997*; *Pollitz et al., 1998*; *Segall et al., 2000*), to develop the depth extent of creep on the northern HF (*Bürgmann et al*., 2000), and to produce distributed−slip models to delineate creeping portions of the Calaveras fault. Where appropriate, we can also formally evaluate variations in the slip patterns with time using a network inversion filter approach (*Segall et al.*, 2000).

The InSAR data set used here has been expanded from 2 interferograms (*Bürgmann et al.*, 2000) to a range−change rate distribution determined from all interferograms included in the 1992−2000 time period (**Figure 8**). GPS velocities now include additional sites, which we began to survey in 1999 in our effort to densify 3D−velocity constraints. The next M6.5+ event along the HF−MF−CF system will likely nucleate near the lower bound of the seismogenic zone, a depth of 8−10 km, where resolution of the slip distribution from surface observations is relatively poor. Constraints from recurrence−determined slip rates at a few depth points offers promise for substantially sharpened resolution near the all−important base of the slipping zone. Even with the high−quality InSAR range−change data available across the northern HF (**Figure 8**), determination of the vertical extent (creep patch depth) and slip rate distribution of the creeping zone is difficult to recover from surface displacements alone for depths greater than about 5 km. **Figure 9** illustrates our approach at the example of the northern HF segment incorporating the updated InSAR results with the creep, repeater and GPS data considered previously (*Bürgmann et al.*, 2000) to determine a distributed slip model. We are now working towards a complete integration of all available data sets along the HF−MF−CF fault system to develop integrated and self−consistent models that rigorously incorporate all the data constraints and uncertainty estimates. Remaining challenges we foresee include the development of a resolution−dependent smoothing constraint, as the quality and amount of data varies significantly along the East Bay faults.

Frictional Modeling of Creeping Faults. In addition to direct inversion of surface displacements for fault slip, we also are developing forward models in which fault slips are not prescribed but solved for using frictional stress boundary conditions. These models solve for slip on a creeping fault as a function of (1) geometry, (2) stress boundary conditions (e.g., distributed or localized shear below the brittle−ductile transition depth, interaction with other faults and remote driving stresses), (3) fault zone properties (i.e., frictional strength) and (3) the distribution of locked patches along the faults (e.g., *Bürgmann et al.*, 2000, *Simpson et al.*, 2001). These models provide a test for the slip inversion results in that they depend on additional constraints provided by the physical properties of the crust and fault zones. We propose to develop our physical models in parallel with the slip inversions with the hope of ultimately developing a mechanically realistic model that satisfies the available data constraints. For this purpose we will continue to rely on the elastic 3D boundary element code (Poly3D) as well as finite element (FEM) modeling using the commercial I−DEAS, a widely used engineering code that has been adapted for use in geodynamical problems by A. Freed (Freed and Lin, 2001), a Berkeley postdoc working on a different project with the PI.

Conclusions/Future

This project is an extension and refinement of our prototype analysis of the northern HF where we incorporated, for the first time, HF subsurface slip rates inferred from recurrence intervals of repeating characteristic microearthquakes into the estimation of the slip distribution on a creeping fault zone based on surface observations of creep, GPS positions and InSAR interferograms (*Bürgmann et al.*, 2000). The proposed work is meant to produce a complete analysis, full integration, and careful interpretation of all available data. This project involves a significantly larger scope than the prototype study with the intent of fully characterizing the distribution of locked and aseismically slipping portions of the hazardous East−Bay fault complex. This effort includes additional work to refine the integration techniques in the slip inversion and to explore the feasibility of monitoring temporal change on these slower slipping faults using both regional NCSN and the low−magnitude−threshold borehole HF data. The slip constraints from all available data are being merged in a formal joint inversion. We have established the feasibility of the approach and the value of using micro−earthquakes for slip−rate monitoring and delineation of subsurface slip on the fault surface. We have significantly increased the datasets that are to be used in the incorporated inversion and have made considerable progress in the development of procedures for integrating the data sets. The project is computationally intensive and identification of repeating sequences has been a laborious task requiring a great deal of individual inspection of waveforms and earthquake relocations at the highest resolution. To expedite this process we are continuing to develop more automated and objective procedures with the eventual goal being quasi−real−time repeater identification and deep slip rate estimation for monitoring slip rate changes at depth and to aid in up to date strain accumulation estimating on locked fault segments. We also hope to have, through other efforts underway, a scanned waveform data base that extends back several decades, providing an opportunity to use the larger events, with proportionally longer recurrence times, to gain insight into the longer term slip process at depth in the Bay area.

To date we have found that the aseismic slip behavior along the partially creeping HF, MF, CF and Quien Sabe Fault is complex both in space and time. We have made further progress in our effort to resolve slip behavior and seismic potential along the East Bay strike−slip faults, as described, and we have searched for and confirmed the existence of dozens of characteristically repeating microearthquake sequences on the southern HF, CF, and MF and shown that their abundance and frequency of repetition relative to other regions such as San Juan Bautista and Parkfield are in proportion to the relative fault slip rates. GPS, creep and InSAR data sets have been developed and continue to grow for most portions of these East−Bay faults, making joint surface−subsurface deformation analyses feasible on them as well. We are continuing to critically evaluate the consistency between the different data sets, examine alternate approaches to resolving sub−surface creep and are carefully studying potential biases in (*Schaff et al.*, manuscript submitted to JGR) and alternate mechanical models for (*Anooshehpoor and Brune*, 2001; *Sammis and Rice*, 2001; *Beeler*, 2001) our repeater−derived slip estimates.

We are continuing the identification of repeating quakes along these faults to densify coverage and temporal resolution, which will better constrain the inferred slip rate estimates they provide. We are in the process of completing formal integration of the expanded repeating quake data set with the GPS and INSAR data on these faults. We are collecting new GPS data to establish site velocities for about 25 stations along the Hayward fault, which were established in 1999. On this expanded scale the dynamics of fault interaction should be easier to define, and sufficient data appear to be present to allow us to characterize and explore the implications of our observed transients in slip rate as has been done on the SAF between Parkfield and San Juan Bautista (*Nadeau and McEvilly*, 1999; 2000). To observe the kinematics of aseismic fault slip at this scale has required regional analysis of thousands of micro−earthquakes and substantial geodetic data sets and the development of improved inversion methods to integrate these data.

Based on the progress we have made to date, we have requested and received from NEHRP additional funding for this project to (1) A complete analysis of all existing ERS−1,2 interferograms (> 150 image pairs) over the San Francisco Bay area, (2) a final round of GPS measurements in 2003 of our East Bay GPS network with data now spanning 3 years for most sites, (3) consistent and integrated micro−earthquake repeater analysis of all 1984−2 3 NCSN catalog events for the HF−MF−CF fault system, (4) analysis of repeating events at lower magnitude from the UCB northern Hayward fault and USGS southern Hayward fault borehole networks, (5) definition of full 3D fault geometry of the HF−MF−CF system from relocated micro−earthquakes, (6) formal slip inversion and rigorous error analysis based on results from tasks (1) − (5), and (7) production of a complete map of the distribution of aseismic slip along the HF−MF−CF system and interpretation of implications for seismic potential and earthquake hazard estimates. The final step of this project will include a careful evaluation of time−varying patterns in the deformation, a rigorous analysis of model assumptions and uncertainties, and evaluation of the results with the goal of improving our theoretical understanding of the physical processes underlying the observed fault slip behavior.

References

Anooshehpoor, A., and J.N. Brune, Quasi−Static Slip−Rate Shielding by Locked and Creeping Zones as an Explanation for Small Repeating Earthquakes at Parkfield, *Bull. Seism. Soc. Am.*, 91, 401−403, 2001.

Beeler, N.M., D.L. Lockner, and S.H. Hickman, A simple stick−slip and creep−slip model for repeating earthquakes and its implications for microearthquakes at Parkfield, *Bull. Seism. Soc. Am.*, 91, 1797−1804, 2001.

Bilham, R., and S. Whitehead, Subsurface creep on the Hayward fault, Fremont, California, *Geophys. Res. Lett.*, *24* (11), 1307−1310, 1997.

Bürgmann, R., R. Arrowsmith, T. Dumitru, and R. McLaughlin, Rise and fall of the southern Santa Cruz Mountains, California, deduced from fission track dating, geomorphic analysis, and geodetic data, *J. Geophys. Res.*, *99* (B10), 20181−20202, 1994.

Bürgmann, R., P. Segall, M. Lisowski, and J. Svarc, Postseismic strain following the 1989 Loma Prieta earthquake from GPS and leveling measurements, *J. Geophys. Res.*, *102*, 4933−4955, 1997.

Bürgmann, R., 1997, Active detachment faulting in the San Francisco Bay area?, *Geology,* v.25, p.1135−1138.

Bürgmann, R., Fielding, E., and Sukhatme, J., 1998a, Slip along the Hayward fault, California, estimated from space−based synthetic aperture radar interferometry, *Geology*, v.26, no. 6, p. 559−562.

Bürgmann, R., J. Sukhatme, and E. Fielding, Seismic potential of the northern Hayward fault from space based SAR imterferometry and GPS measurments, 1998b, *EOS Trans. AGU*, *79* (45), 36.

Bürgmann, R., D. Schmidt, R.M. Nadeau, M. d'Alessio, E. Fielding, D. Manaker, T.V. McEvilly, and M.H. Murray, Earthquake Potential along the Northern Hayward Fault, California, *SCIENCE*, 289, 1178−1182, 2000.

Ferretti, A., C. Prati & F. Rocca (2000). Permanent scatterers in SAR interferometry, *manuscript in preparation* Galehouse, J.S., Theodolite measurements of creep rates on San Francisco Bay region faults, *U.S. Geol. Surv. Open File Rep.*, *95−210*, 335−346, 1995.

Freed, A.M., and J. Lin, Delayed triggering of the 1999 Hector Mine earthquake by viscoelastic stress transfer, *Nature*, 411, 180−183, 2001.

Harris, R., and P. Segall, Detection of a locked zone at depth on the Parkfield, California segment of the San Andreas fault, *J. Geophys. Res.*, *92*, 7945−7962, 1987.

Johanson, I.A., and R. Bürgmann, Using point measurements from InSAR to detect transient deformation, *Eos Trans. AGU*, *91*, xxx, 2001.

Jones, D.L., R. Graymer, C. Wang, T.V. McEvilly and A. Lomax, Neogene transpressive evolution of the California coast ranges, *Tectonics*, 13, 561−574, 1994.

Kelson, K.I., G.D. Simpson, W.R. Lettis, and C.C. Haraden, Holocene slip rate and earthquake recurrence of the northern Calaveras fault at Leyden Creek, California, *J. Geophys. Res.*, *101*, 5691−5705, 1996.

Langbein, J., R.L. Gwyther and M.T. Gladwin, Possible increase in fault slip rate at Parkfield in 1993 as inferred from deformation measurements from 1986 to 1997, *Seism. Res. L.*, 69, 151, 1998.

Langbein, J. O., R. O. Burford, L. E. Slater, Variations in fault slip and strain accumulation at

Parkfield, California; initial results using two−color geodimeter measurements, 1984−1988, *J. Geoph. Res.*, 95, 2533, 1990
Lienkaemper, J.J., G. Borchardt, and M. Lisowski, Historic creeprate and potential for seismic slip along the Hayward Fault, California, *J. Geophys. Res.*, *96*, 18261−18283, 1991.
Lienkaemper, J.J., J.S. Galehouse, and R.W. Simpson, Creep response of the Hayward fault to stress changes caused by the Loma Prieta earthquake, *Science*, *276*, 2014−2016, 1997.
Lienkaemper, J.J., J.S. Galehouse, and R.W. Simpson, Long−term monitoring of creep rate along the Hayward fault and evidence for a lasting creep response to 1989 Loma Prieta earthquake, *Geophys. Res. Lett.*, *28*, 2265−2268, 2001.
Linde, A. T., M. T. Gladwin, M. J. S. Johnston, *et al.* (1996). A slow earthquake sequence on the San Andreas fault, *Nature* 383, 65−68.
Murray, M.H., J.C. Savage, M. Lisowski, and W.K. Gross, Coseismic displacements: 1992 Landers, California, earthquake, *Geophys. Res. Lett.*, 20, 623−626, 1993.
Murray, M. H., Marshall, G. A., Lisowski, M., and Stein, R. S., The 1992 M=7 Cape Mendocino, California, earthquake: Coseismic deformation at the south end of the Cascadia megathrust, *J. Geophys. Res.*, 17,707−17,725, 1996.
Nadeau, R.M., M. Antolik, W. Foxall, P.A. Johnson, and T.V. McEvilly, Seismological Studies at Parkfield III: Microearthquake Clusters in the Study of Fault−Zone Dynamics, *Bull. Seism. Soc. Am.*, 84, 247−263, 1994.
Nadeau, R.M., W. Foxall, and T.V. McEvilly, Clustering and Periodic Recurrence of Microearthquakes on the San Andreas Fault at Parkfield, California, *Science,* 267, 503−507, 1995.
Nadeau, R.M. (1995). Characterization and application of microearthquake clusters to problems of scaling, fault zone dynamics, and seismic monitoring at Parkfield, California, *Ph.D. Thesis*, University of California, Berkeley, 200 pp.
Nadeau, R. M. and T. V. McEvilly, Seismological Studies at Parkfield V: Characteristic microearthquake sequences as fault−zone drilling targets, *Bull. Seism. Soc. Am.*, 87, 1463−1472, 1997.
Nadeau, R. M. and L. R. Johnson, Seismological Studies at Parkfield VI: Moment Release Rates and Estimates of Source Parameters for Small Repeating Earthquakes, *Bull. Seism. Soc. Am.*, 88, 790−814, 1998.
Nadeau, R. M. and T. V. McEvilly, The Parkfield Experiment: A New View of Fault−Zone Process, *Seism. Res. L.*, 69, 151, 1998a.
Nadeau, R. M. & T. V. McEvilly (1999). Fault slip rates at depth from recurrence intervals of repeating microearthquakes, *Science* 285, 718−721.
Nadeau, R.M. and T.V. McEvilly, Spatial and Temporal Heterogeneity of Fault Slip on the San Andreas Fault System in Central California, *Seism. Res. Lett.*, 71, 263, 2000.
Okada, Y., Surface Deformation due to shear and tensile faults in a half−space, *Bull. Seism. Soc. Am.*, 75, 1135−1154, 1985.
Pollitz, R., R. Burgmann, and P. Segall, Joint estimation of afterslip rate and postseismic relaxation following the 1989 Loma Prieta earthquake, *J. Geophys. Res.*, 103, 26,975−26,992, 1998.
Sammis, C.G, and R.J. Rice, Repeating earthquakes as low−stress drop events at a border between locked and creeping fault patches, *Bull. Seism. Soc. Am.* 91, 532−537, 2001.
Savage, J.C., and M. Lisowski, Inferred depth of creep on the Hayward fault, central California,

J. Geophys. Res., *98*, 787−795, 1992.
Schmidt, D.A., and Bürgmann, R., Temporal slip rate response of the Hayward fault to static stress perturbations using a rate and state constitutive law, *EOS Trans. AGU*, *79* (45), 607, 1998.
Segall, P., R. Burgmann, and M. Matthews, Time dependent deformation following the 1989 Loma Prieta earthquake, *J. Geophys. Res.*, 105, 5615−5634, 2000.
Schmidt, D.A., R. Bürgmann, and S.A. Lawrence, Imaging time−dependent fault creep and basin subsidence in the San Francisco Bay Area using InSAR, *Eos Trans. AGU*, *81*, 336, 2000.
Simpson, R.W., J.J. Lienkaemper, and J.S. Galehouse, Variations in creep rate along the Hayward fault, California, interpreted as changes in depth of creep, *Geophys. Res. Lett.*, *28*, 2269−2272, 2001.
Templeton, D.C., R.M. Nadeau and R. Bürgmann, Structure and kinematics at the juncture between the San Andreas and southern Calaveras faults, *Eos Trans. AGU*, 82, F881, 2001.
Toppozada, T.R., and G. Borchardt, Re−evaluation of the 1836 "Hayward fault" and the 1838 San Andreas fault earthquakes, *Bull. Seism. Soc. Am.*, *88*, 140−159, 1998.
Waldhauser, F., W.L. Ellsworth, A. Cole, Slip−Parallel Seismic Lineations on the Northern Hayward Fault, California, *Geophys. Res. Lett.*, 26, 3525, 1999.
Wilber, M.M., and Bürgmann, R., Slip behavior at depth on the Pajaro segment of the San Andreas fault, California, *EOS Trans. AGU*, *80* (17), 330, 1999.
Williams, P.L., Geologic record of southern Hayward fault earthquakes, *Div. Mines Geol. Spec. Pub.*, *113*, 171−179, 1992.
Yu, E., and P. Segall, Slip in the 1868 Hayward earthquake from the analysis of historical triangulation data, *J. Geophys. Res.*, *101* (B7), 16,101−16,118, 1996.
Uhrhammer, R.A., Broadband near−field moment tensor inversion, *EOS*, 73, 375, 1992.
Working Group on California Earthquake Probabilities (WGCEP), Probability of large earthquakes in the San Francisco Bay Region, California, *U.S. Geol. Surv. Circ.*, *1053*, 1−51, 1990.
Working Group on California Earthquake Probabilities (WGCEP), Earthquake Probabilities in the San Francisco Bay Region: 2000 to 2030, *Open File Report 99−127*, 1999.

Bibliography

Burgmann, R., D. Schmidt, R.M. Nadeau, M. d'Alessio, E. Fielding, D. Manaker, T.V. McEvilly, and M.H. Murray, Earthquake Potential along the Northern Hayward Fault, California, *Science*, 289, 1178−1182, 2000.

McEvilly, T.V. and R.M. Nadeau, (Invited) Deformation Process in a Seismogenic Fault Zone from High−Resolution Studies of Microearthquake Occurrence, *GSA abstracts with Programs*, 31, May, 1999.

Nadeau, R.M. and T.V. McEvilly, (Invited) Cluster Signature Analysis of Earthquakes on Central San Andreas and Bay Area Faults, *EOS Trans., AGU*, 80, F690, 1999.

Nadeau, R.M., L.R. Johnson, H.−R. Wenk, and T.V. McEvilly, Source dimensions of small earthquakes, *EOS Trans., AGU*, 80, F682, 1999.

Nadeau, R.M., Repeating Small Earthquakes at Parkfield CA, *11th Annual IRIS Workshop*, June 9−12, 1999, Tenaya Lodge at Yosemite, Fish Camp, CA

Nadeau, R.M. and T.V. McEvilly, Fault Slip and Loading Rates at Depth from Recurrence Intervals of Repeating Microearthquakes, *Seism. Res. Lett.*, 70, 236, 1999.

Nadeau, R.M., and T.V. McEvilly, Fault slip rates at depth from recurrence intervals of repeating microearthquakes. *Science*, 285, 718−721, 1999.

Nadeau, R.M. And T.V. McEvilly, Spatial and Temporal Heterogeneity of Fault Slip from Repeating Micro−Earthquakes along the San Andreas Fault in Central California, *EOS Trans., AGU*, 81, F919, 2000.

Nadeau, R.M. and T.V. McEvilly, Spatial and Temporal Heterogeneity of Fault Slip on the San Andreas Fault System in Central California, *12th Annual IRIS Workshop*, May7−11, 2000, Samoset Resort, Rockport, Maine.

Nadeau, R.M. and T.V. McEvilly, Spatial and Temporal Heterogeneity of Fault Slip on the San Andreas Fault System in Central California, *Seism. Res. Lett.*, 71, 263, 2000.

Nadeau, R.M. And T.V. McEvilly, Deformation Process of the Central SAF from High−Resolution Studies of Microearthquakes, *3rd Conference on Tectonic Problems of the San Andreas Fault System*, *Stanford University*, *Stanford*, *CA*, September 6−8, 2000.

Schmidt, D.A., Burgmann, R., and Kenner, S.J., Induced left−lateral creep on the Hayward fault following the 1906 San Francisco earthquake, *EOS Trans. AGU*, 80 (17), 324, 1999.

Schmidt, D.A., R. Burgmann, and S.A. Lawrence, Imaging time−dependent fault creep and basin subsidence in the San Francisco Bay Area using InSAR, *Eos Trans. AGU*, 81, 336, 2000.

Templeton, D.C., R.M. Nadeau and R. Bürgmann, Structure and kinematics at the juncture between the San Andreas and southern Calaveras faults, *Eos Trans. AGU*, 82, F881, 2001.

Working Group on California Earthquake Probabilities, Earthquake Probabilities in the San Francisco Bay Region: 2000 to 2030, *Open File Report 99−517*, 1999.

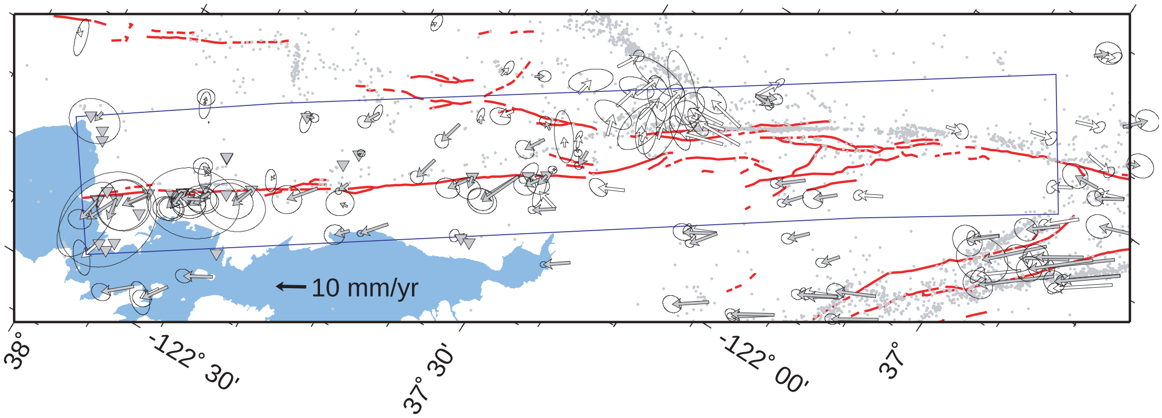

Figure 1. Map of horizontal site velocities along the HF-MF-CF system in an oblique Mercator projection parallel to the relative motion between the Pacific plate and the SNGV microplate. Grey arrows are GPS velocities from 1991 - 2001 (though many stations have much shorter observation durations) relative to station BRIB and their 95% confidence ellipses. Grey triangles are sites where we have 1 - 3 years worth of GPS observations but are not yet able to determine well constrained velocities. White arrows are EDM derived velocities from 1970 - 1997 in the same reference frame as the GPS data. On going additional measurements will significantly improve the data quality, and ability to resolve fault slip model parameters. Also shown are 1984-2002 earthquakes (gray dots), relocated with hypoDD within the blue box along the East Bay fault system. Outside the boxed area, locations come from the NCSN catalog and have location errors on the order of 1.5 km.

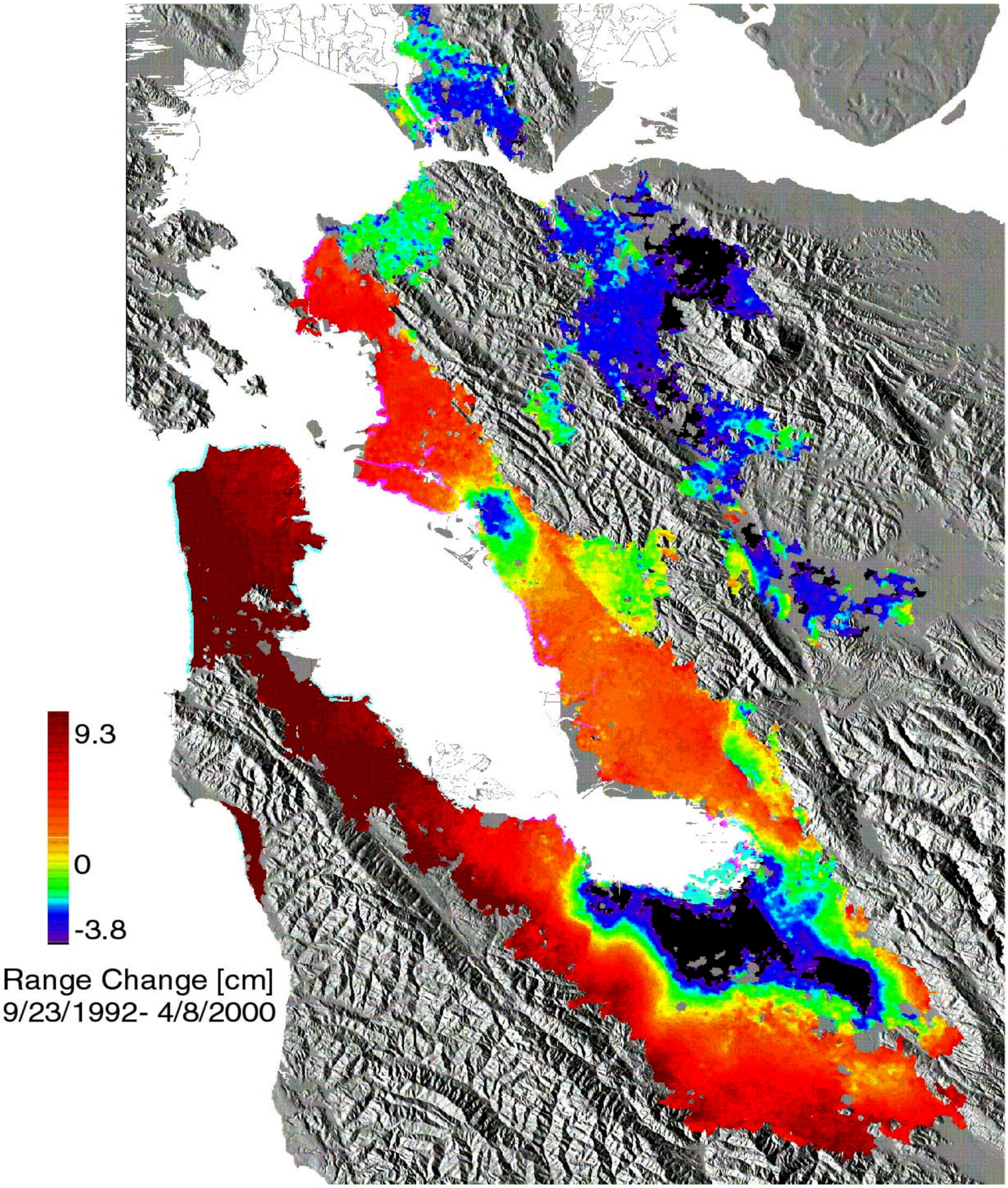

Figure 2. A differential interferogram of the San Francisco Bay Area shows the crustal deformation over a 7.5 year period. Superimposed over a shaded relief image is the change in range along the look direction of the satellite. Surface creep on the Hayward fault is represented by a discontinous jump in phase observed in Pinole, Castro Valley, and Fremont. The Interseismic strain profile across the Bay Area related to deformation across the plate boundary is represented by the gradient from red to blue. Coherent data is primarily limited to developed regions where surface properties do not significantly change with time.

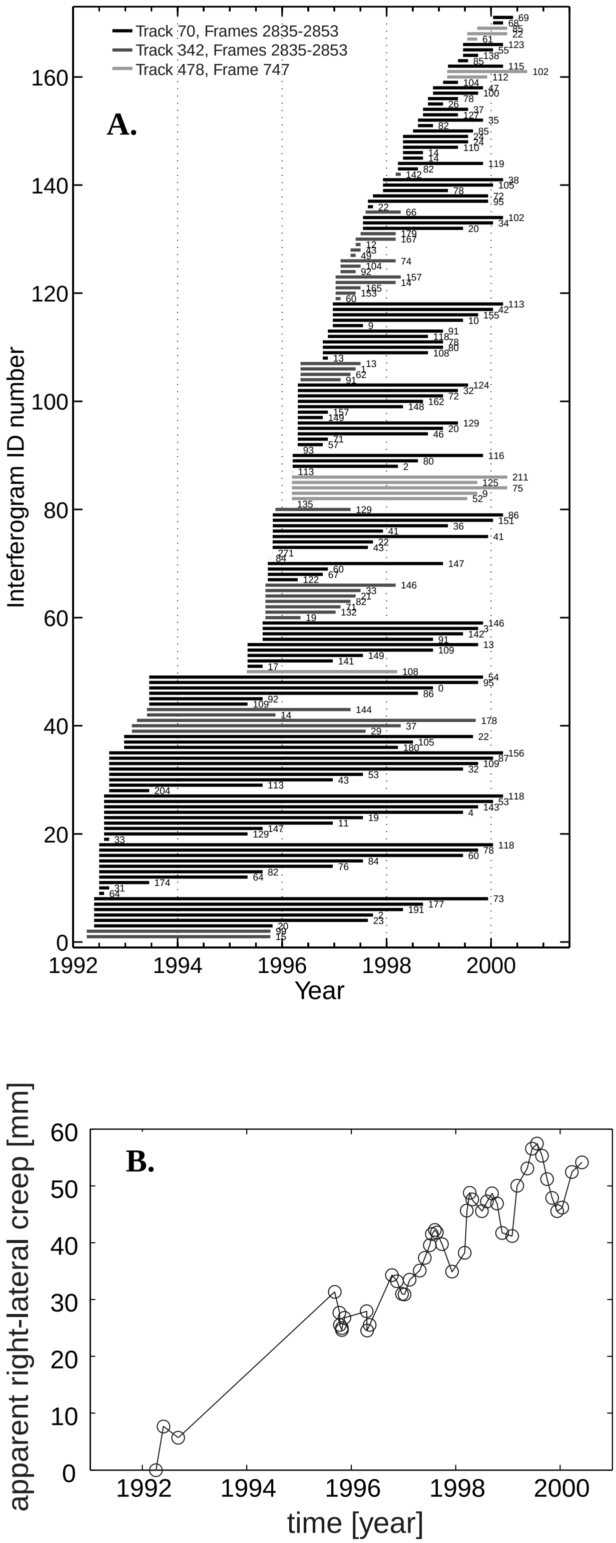

Figure 3. (A) A graphical list of interferograms shows the complete list of processed InSAR data for the Bay Area. 87 SAR scenes have been used to produce 171 interferograms with perpendicular baselines of less than ~200 m. The different shades of gray represent SAR data collected along different orbital tracks. The perpendicular baseline, in meters, for a given interferogram is shown to the right of each horizontal bar. (B) The information contained in all the interferograms is synthesized into an InSAR time series using a least-squares inversion. The time dependent surface creep is shown near Point Pinole. The time series analysis suggests a surface creep rate of 6.3+/-0.4 mm/yr across a 1 km baseline.

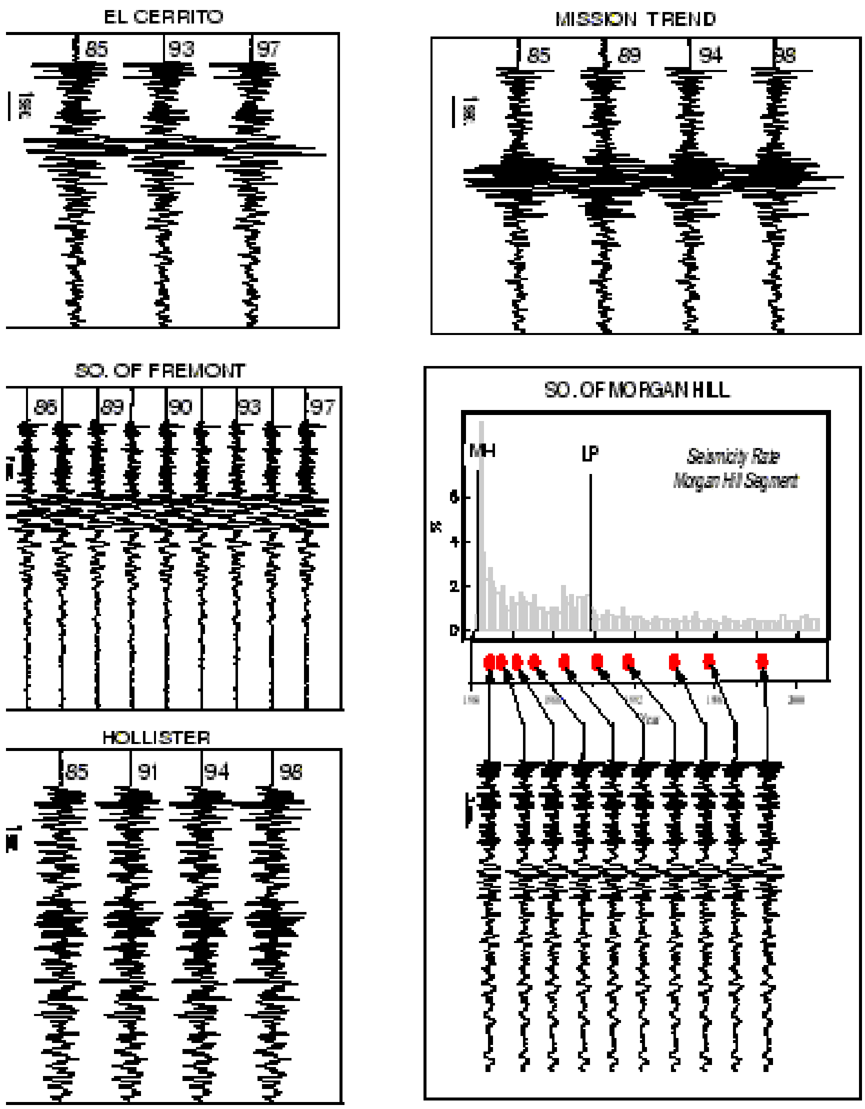

Figure 4. Example repeating sequences along the Hayward, Calaveras and Mission faults. Characteristic repeaters are numerous, widespread anddistributed in time for all the regions examined so far. Variations in the rates of repetition are consistent with known variations in slip rate both along strike and through time. For example, sequences NW of morgan Hill (MH) typically show a steadily decreasing repeat rate with time since the 1984 MH magnitude 6. We also plan on examining changes in repeat rates and micro-quake inferred slip as they relate to the occurrence of Loma Prieta (LP) and other significant near by events.

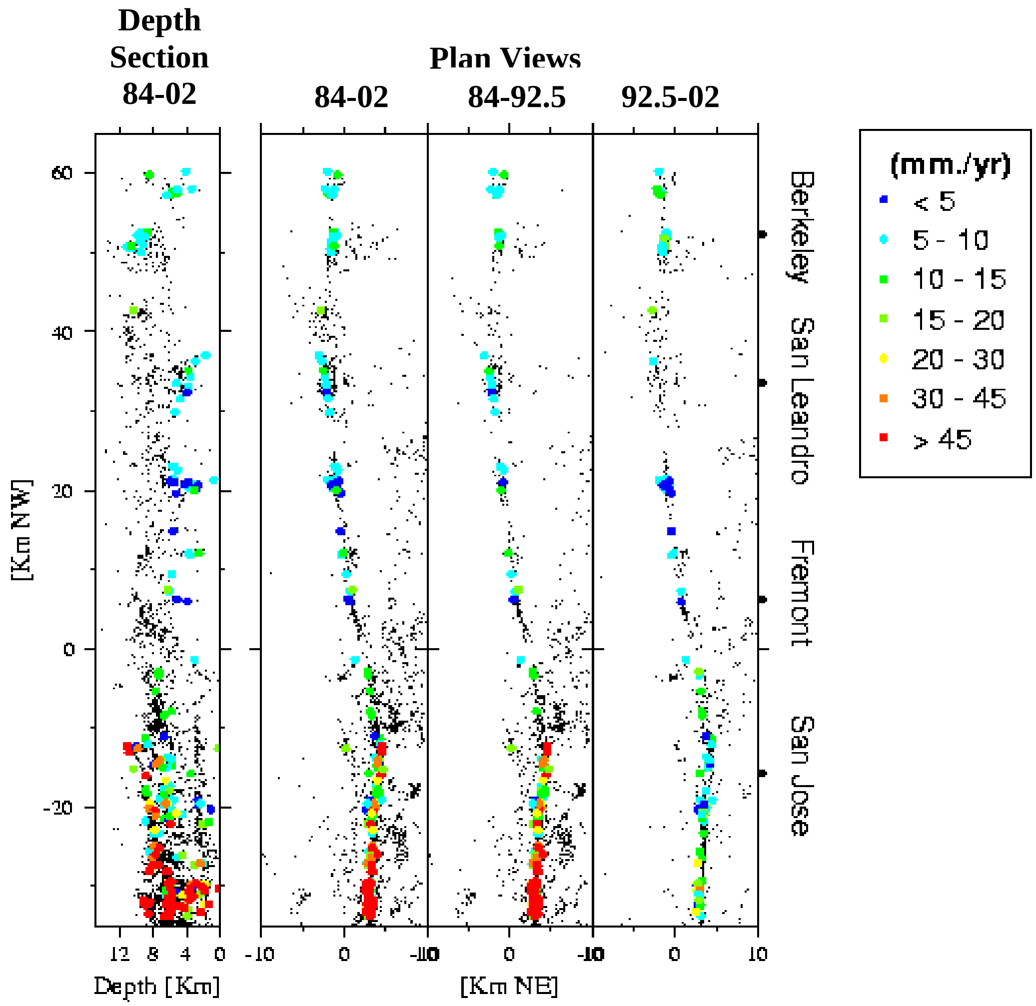

Figure 5. Point fault slip rate estimates at depth inferred from recurrence intervals of characteristic micro-earthquakes, superposed on the HypoDD-relocated seismicity along a 120-km-long stretch of the Hayward (HF), Mission (MF) and Calaveras (CF) faults. Rates of slip in mm/yr are coded by color as indicated. Each color point represents the average slip rate between time sequential pairs of characteristic events in a sequence. Left panel shows, in depth section, all slip rate pair estimates and background seismicity for the time period 1984-2002. Second panel shows the same data in map view. Panel three (second from right) shows data in map view for pairs occurring between 1984 to 1992.5, and far left map shows similar data for the period 1992.5 to 2002.2. A time variable slip rate is clear, particularly along the CF where slip rates are high following the 1984 Morgan Hill main shock and slow down significantly afterwards. Slip rate is lowest on the southern HF and MF trends. On these segments, below about 5-6 km, characteristically repeating sequences are absent while background seismicity can clearly be seen. This suggests that the boundary separating the repeating and non-repeating regions often delineates the boundary between creeping and non-creeping (locked) fault behavior at depth.

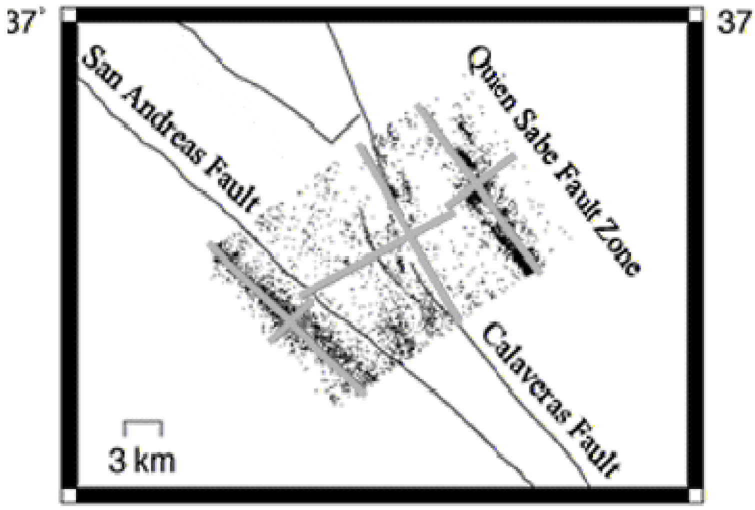

Figure 6. Location map. Map of study area near bifurcation region of the San Andreas, Calaveras and Quien Sabe Faults. Shown are the surface fault traces and local seismicity from 1984 to 2001 and the location of fault sections shown in **Figure 7**.

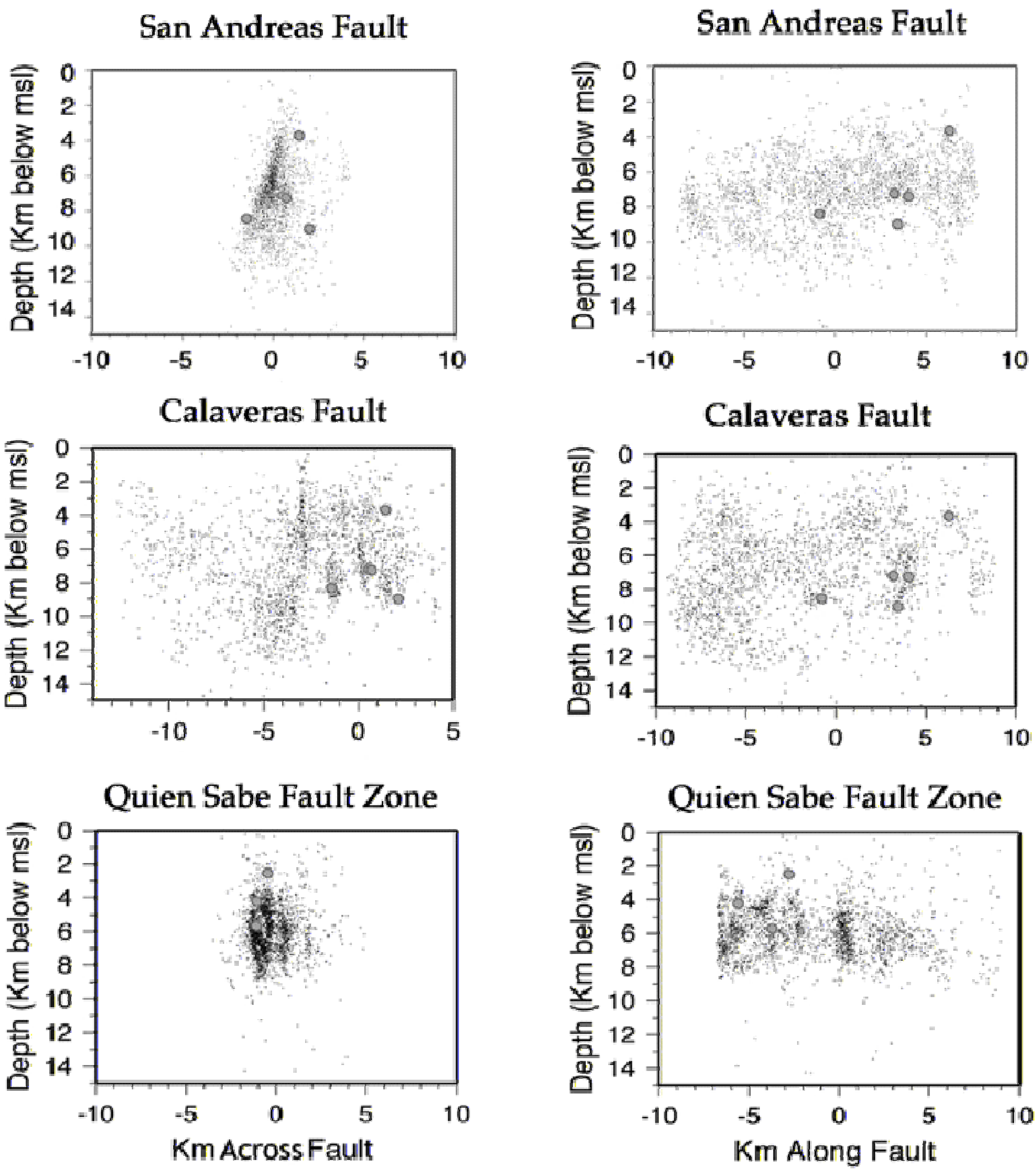

Figure 7. Cross sections corresponding to **Figure 6**. Locations of repeating earthquake sequences, indicated by the gray filled circles, shown with respect to background seismicity for the San Andreas, Calaveras and Quien Sabe fault Zone. Fault perpendicular cross sections are to the left and fault parallel cross sections to the right.

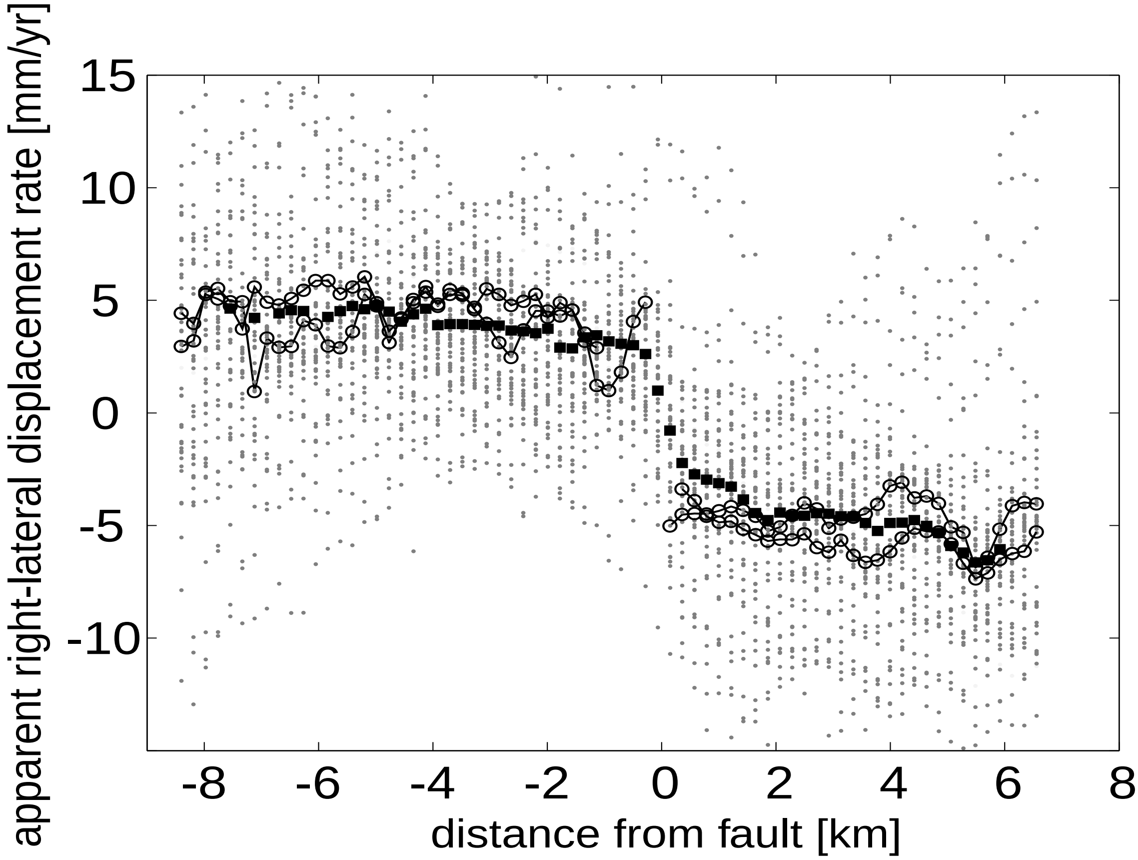

Figure 8. Profiles of InSAR range change data across the northern Hayward fault. Circles indicate the 2 interferograms used in *Bürgmann et al.* (2000). Scattered gray dots are all interferograms available. Solid squares are the combined range- change estimates from all the data (see **Figure 3B**).

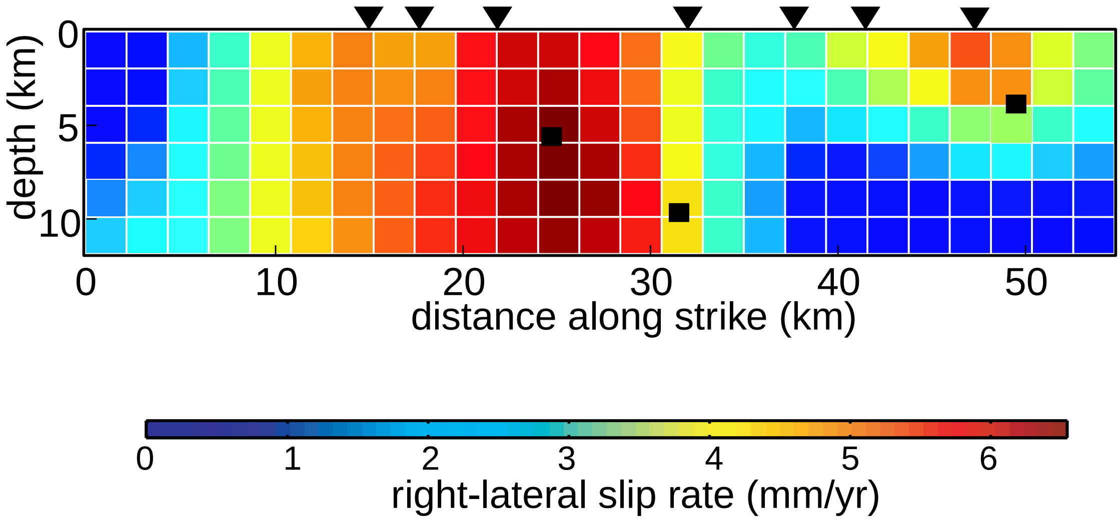

Figure 9. NW-SE section of preliminary distributed-slip inversion of (1) regional GPS data, (2) combined InSAR range-change data across the NHF, (3) surface creep measurements and (4) sub-surface aseismic slip rate estimates from repeating microearthquakes. Slip is constrained to go towards zero under San Pablo Bay. Locations of surface creep measurements (*Lienkaemper et al.*, 2001) are indicated by triangles and the location of subsurface repeater clusters (Bürgmann et al., 2000) are shown as squares.